Proceedings of the DIS'2004, Štrbské Pleso, Slovakia

DEEPLY VIRTUAL COMPTON SCATTERING IN THE SATURATION APPROACH

LAURENT FAVART*, M.V.T. MACHADO **
* I.I.H.E., Université Libre de Bruxelles, Belgium
E-mail: lfavart@ulb.ac.be
** High Energy Physics Phenomenology Group, GFPAE, IF-UFRGS
Caixa Postal 15051, CEP 91501-970, Porto Alegre, RS, Brazil
E-mail: magnus@if.ufrgs.br

1 Introduction

The study of hard exclusive reactions in the Bjorken limit is crucial to obtain information on parton dynamical correlations in the nucleon. The recent data from DESY *ep* collider HERA on exclusive diffractive virtual Compton process [1,2,3] (DVCS) at large Q^2 becomes an important source to study the partons, in particular gluon, inside the proton for non-forward kinematics and its relation with the forward one. A considerable interest of the DVCS process comes from the particular access it gives to these generalized parton distributions (GDP) through the interference term with the Bethe-Heitler process. On the other hand, recently the color dipole formalism has been provided a simultaneous description of photon induced process. The inclusive deep inelastic reaction and the photon diffractive dissociation has been successfully described and the study of other exclusive process as DVCS is an important test of the color dipole approach. The work reported here, summarizing the studies in Refs. [4,5], applies the successful saturation model [6] to the DVCS process. The model interpolates between the small and large dipole configurations and has its parameters obtained from an adjust to small x HERA data. Moreover, its QCD evolution has been recently computed [7], which improves the high Q^2 data description.

2 DVCS cross section in the color dipole picture

Based on the color dipole framework, the DVCS process can be seen as a succession in time of three factorisable subprocesses: i) the photon fluctuates in a quark-antiquark pair, ii) this color dipole interacts with the proton target, iii) the quark pair annihilates in a real photon. As usual, the kinematic variables are the c.m.s. energy squared $s = W_{\gamma p}^2 = (p+q)^2$, where p and q are the proton and the photon momenta respectively, the photon virtuality squared $Q^2 = -q^2$ and the Bjorken scale $x = Q^2/(W_{\gamma p}^2 + Q^2)$. The DVCS imaginary part of the amplitude at zero momentum transfer reads as,

$$\mathcal{I}m\,\mathcal{A}\,(s, Q^2, t=0) = \int_0^1 dz \int d^2\boldsymbol{r}\,\Psi_T^*(z,\boldsymbol{r},\,Q_1^2=Q^2)\,\Psi_T(z,\boldsymbol{r},\,Q_2^2=0)\,\sigma_{dip}(\tilde{x},\boldsymbol{r}^2)\,,$$

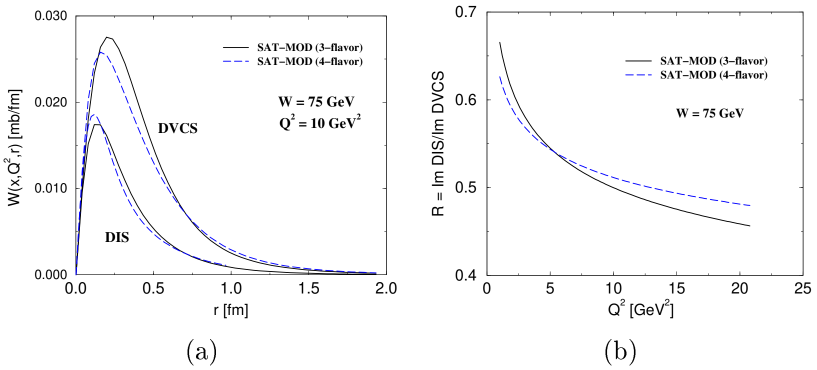

Figure 1. **(a)** *Comparison between the profile function $W(\boldsymbol{r}, Q^2)$ as a function of the dipole size $\boldsymbol{r}$ for DVCS and inclusive DIS processes at $Q^2 = 10\ GeV^2$.* **(b)** *The ratio of the imaginary parts of the DIS and DVCS amplitudes as a function of Q^2 at $W = 75\ GeV$.*

where $\sigma_{dip}(\tilde{x}, \boldsymbol{r}^2)$ is the dipole cross section, which depends on the scaling variable $\tilde{x} = \frac{Q^2+4m_f^2}{(W_{\gamma p}^2+Q^2)}$ and dipole size, $\boldsymbol{r}$. The product of the photon wavefunctions (transverse polarization) is given by,

$$\Psi_T^* \, \Psi_T = \frac{6\alpha_{\mathrm{em}}}{4\,\pi^2} \sum_f e_f^2 \, \left[f(z)\, \varepsilon_1 \, K_1(\varepsilon_1 \, r)\, \varepsilon_2 \, K_1(\varepsilon_2 \, r) + m_f^2 \; K_0(\varepsilon_1 \, r)\, K_0(\varepsilon_2 \, r) \right] \, ,$$

where $\varepsilon_{1,\,2}^2 = z(1-z)\, Q_{1,\,2}^2 + m_f^2$ and $f(z) = [z^2 + (1-z)^2]$. The quark mass, m_f, plays the role of a regulator as $Q^2 \to 0$. The relative contributions from dipoles of different sizes can be analyzed with the weight (profile) function,

$$W(\boldsymbol{r}, Q^2) = \int_0^1 dz \, \boldsymbol{r} \; \Psi_T^*(z, \, \boldsymbol{r}, \, Q_1^2 = Q^2) \, \Psi_T(z, \, \boldsymbol{r}, \, Q_2^2 = 0) \, \sigma_{dip} \, (\tilde{x}, \, \boldsymbol{r}^2) \, .$$

In the DIS process the contribution of large dipole configurations is observed to diminish in a sizable way as the virtualities increase. However, as shown in Fig. (1-a), the DVCS profile selects larger dipole sizes in contrast to the inclusive DIS case, even at relatively large Q^2 (similar result has been obtained in Ref.[8]). The calculation was performed using the saturation model [6] for both three and four-flavor analysis. The inclusion of the charm content gives a lower normalization for the profile and by consequence for the total cross section. The impact of the charm is smaller in the inclusive DIS case than in DVCS process, confirming that DVCS is more sensitive to the non-perturbative (soft) content of the scattering process. Moreover, in order to estimate the importance of the skewing effect, we calculate the ratio between the imaginary parts of the forward $t = 0$ amplitudes for DIS and DVCS, R $= \mathcal{I}m$ DIS$/\mathcal{I}m$ DVCS. As shown in Fig. (1-b) our result presents values slightly above those from an aligned jet model analysis in Ref. [9] and below those from the dipole analysis in Ref. [8].

The final expression for the DVCS cross section is written as,

$$\sigma(\gamma^* \, p \to \gamma \, p) = \frac{[\, \mathcal{I}m \, \mathcal{A}(s, Q^2, t = 0)\,]^2}{16\, \pi \, B} \, (1 + \rho^2) \, ,$$

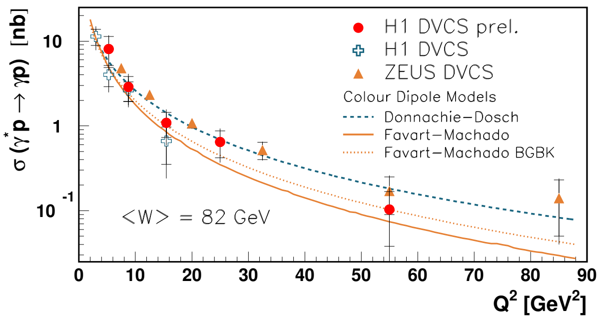

Figure 2. *The photon level DVCS cross section as a function of virtuality Q^2 at $W = 75$ GeV. Data are compared to the present prediction, with and without (BGBK) QCD evolution (see text).*

where B is the t slope parameter and comes from a simple exponential parameterization and ρ, the ratio between the real to imaginary part, is computed according to the dispersion relations (more details in Ref. [4]).

3 Cross section comparison to Data

In what follows we present the results for the phenomenological saturation models and also its version considering QCD evolution [7] (labeled BGBK), giving the dipole cross section gluon dependent. In Fig. 2 (from the H1 conference paper [3]) one compares their prediction with the existing measurement from H1 and ZEUS Collaborations [1,2,3]. The color dipole prediction from Donnachie-Dosh [10] is also presented for the sake of comparison. As the B value has never been measured for DVCS, the normalization of the theoretical prediction is basically free (usually values of $5 < B < 9$ GeV^{-2} are considered, and the fixed value of $B = 7$ GeV^{-2} is chosen on the figure).

Although there is a little difference of normalization between H1 and ZEUS measurements, which makes difficult to set an overall B value for all measurements, the behavior on Q^2 and W (see Ref. [3]) is well reproduced. On the other hand, for $Q^2 \gtrsim 40$ GeV^2 our prediction still underestimates the experimental data. This change of behavior in the Q^2 shape can indicate two situations: (a) the B slope would diminish as increasing virtualities or; (b) some additional effect should appear at higher Q^2. In order to investigate the first hypothesis, we compute cross section using a Q^2 dependent slope: $B(Q^2) = 8[1 - 0.15\ln(Q^2/2)]$ GeV^{-2} (see Ref. [5] for details). Concerning the second hypothesis, we have investigated two options: QCD evolution (using BGBK model) and skewedness effects. For the skewedness corrections, the ratio of off-forward to forward gluon distribution are are given explicitly by [11], $R_g\,(Q^2) = \frac{2^{2\lambda+3}}{\sqrt{\pi}}\,\frac{\Gamma\left(\lambda+\frac{5}{2}\right)}{\Gamma\,(\lambda+4)}$, where λ is the effective power on energy of the scattering amplitude. For our purpose the amplitude is multiplied by R_g, in order to estimate the size of the skewedness effects.

To compare the Q^2 dependence, we normalize all models to describe the ZEUS data point at the lowest Q^2 value. Further, we plot the ratio of each model to

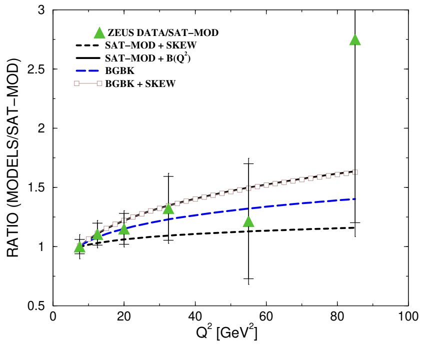

Figure 3. *The ratio MODELS/SAT-MOD as a function of Q^2 (see text for details).*

our baseline model SAT-MOD as a function of Q^2. Such a procedure allows a Q^2 dependence comparison independently of the normalization effect. These ratios are shown in Fig. 3, where the points (triangles-up) are the ratio of the ZEUS data to SAT-MOD including the error bars for the statistical (inner) and sum in quadrature of statistical and systematic (outer) uncertainties.

We verify that several models can account for the measured Q^2 dependence, which are not distinguishable with the present experimental precision. If the change in normalization is small for the inclusion of a Q^2 dependence in B, the effect is of the order of 12% for BGBK with respect to the basic SAT-MOD and of 40% for the skewedness effect (SKEW) and still larger when the different effect are combined (60% for BGBK+SKEW). Therefore, these issues show clearly the importance of a measurement of the slope B. Such a measurement would already allow to discriminate among the different theoretical predictions with an amount of data comparable to the present ZEUS measurement.

References

1. C. Adloff *et al.* [H1 Collaboration], Phys. Lett. B **517** (2001) 47.
2. S. Chekanov *et al.* [ZEUS Collaboration], Phys. Lett. B **573**, 46 (2003).
3. L. Favart, in EPS 2003 - High Energy Physics conference (HEP). Eur. Phys. J. C **33** , s01 (2004) s509, [arXiv:hep-ex/0312013].
4. L. Favart and M. V. T. Machado, Eur. Phys. J. C **29** (2003) 365.
5. L. Favart and M. V. T. Machado, Eur. Phys. J. C **34** (2004) 429.
6. K. Golec-Biernat and M. Wusthoff, Phys. Rev. D **59** (1999) 014017.
7. J. Bartels, K. Golec-Biernat and H. Kowalski, Phys. Rev. D **66** (2002) 014001.
8. M. McDermott, R. Sandapen and G. Shaw, Eur. Phys. J. C **22** (2002) 655.
9. L. L. Frankfurt, A. Freund and M. Strikman, Phys. Rev. D **58**, 114001 (1998).
10. A. Donnachie and H. G. Dosch, Phys. Lett. B**502** (2001) 74.
11. A. G. Shuvaev *et al.*, Phys. Rev. D **60**, 014015 (1999).